

# NUMERICAL MODELLING OF THE WEDGE SPLITTING TEST IN ROCK SPECIMENS, USING FRACTURE-BASED ZERO-THICKNESS INTERFACE ELEMENTS

J. LIAUDAT<sup>\*</sup>, D.GAROLERA<sup>\*</sup>, A. MARTÍNEZ<sup>\*</sup>, I. CAROL<sup>\*</sup>,

M.R. LAKSHMIKANTHA<sup>†</sup> AND J. ALVARELLOS<sup>♠</sup>

<sup>\*</sup>Dept. of Geotechnical Engineering and Geo-Sciences  
Universitat Politècnica de Catalunya. BarcelonaTech (UPC).  
Campus Nord UPC, 08034 Barcelona, Spain  
e-mail: ignacio.carol@upc.edu

<sup>†</sup>Repsol Technology Hub  
The Woodlands, TX 77381, USA  
e-mail: m.lakshmikantha@repsol.com

<sup>♠</sup>Centro de Tecnología de Repsol  
28935 Móstoles (Madrid)  
e-mail: jose.alvarells@repsol.com

**Key words:** Rock, WST, Fracture Mechanics, FEM, Interface Elements

**Abstract.** The purpose of the Wedge Splitting Test (WST) is to generate stable mode I fracture crack along a pre-established path, and be able to measure the specific fracture energy parameter of the material  $G_F^I$ . The test is performed on standard cylindrical notched specimens. In order to make decision on the optimal notch geometry for a specific rock test, a number of WST experiments were simulated numerically via FEM. Continuum elements with isotropic elastic behavior were used to represent the rock, the steel loading plates and an “equivalent spring” to the testing machine compliance. The notch and the fracture path on the rock were represented via zero-thickness interface elements. The notch elements were assumed linear elastic with very low elastic stiffness parameters  $K_n$  and  $K_t$ , so that they do not oppose any significant resistance to opening. The constitutive model used for the interface elements along the fracture path was the elastoplastic constitutive formulation with fracture energy-based evolution laws. The model results match very realistically the curves obtained in the experimental WST, allowing us to estimate indirectly, not only the specific fracture energy but also other basic mechanical parameters of the rock, such as the elastic modulus and the tensile strength.

## 1 INTRODUCTION

The Wedge Splitting Test (WST) is a method to generate stable fracture propagation in quasi-brittle materials, e.g. rock or concrete, in order to determine fracture mechanics

parameters in mode I such as the fracture toughness ( $K_{Ic}$ ) for the linear theory, or the specific fracture energy ( $G_f^I$ ) for the non-linear theory [1,2].

The method uses cylindrical or prismatic specimens in which a notch has been cut in order to prefigure the cracking path. A pair of steel loading plates equipped with roller bearings is glued to both sides of the notch mouth, and lateral opening displacement of the rollers is imposed through a wedge moving vertically down in order to create a stable crack growth. From the splitting force – average Crack Opening Displacement (COD) response of the specimen, the specific fracture energy is determined. For fracture toughness evaluation, a series of unload-reload cycles is necessary.

In this paper, a finite element model based on zero-thickness interface elements is used to simulate the WST and estimate indirectly, not only the specific fracture energy but also other basic mechanical parameters of the rock, such as the elastic modulus and the tensile strength.

## 2 WEDGE SPLITTING TESTS

### 2.1 Principles

A scheme of the test setup and a free body diagram of forces on the wedge are shown in Figure 1, taken from [3]. The horizontal force applied to the specimen ( $P_H$ ) is calculated by means of Equation (1), where  $P_V$  is the vertical load applied,  $\theta$  is the wedge angle and  $\mu$  is the coefficient of friction between wedge and roller.

$$P_H = \frac{1 - \mu \tan \theta}{2(\mu + \tan \theta)} P_V \quad (1)$$

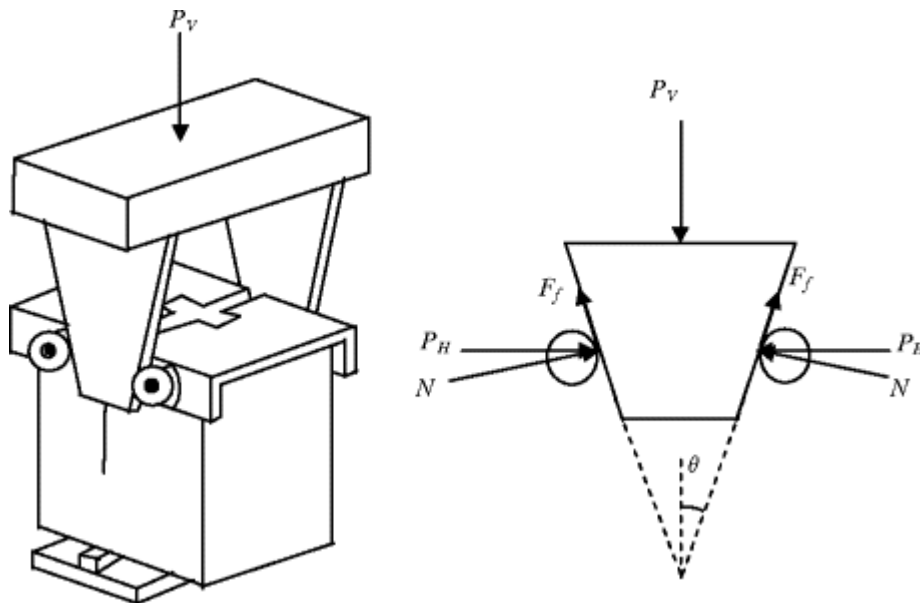


**Figure 1:** Details of the wedge splitting test (WST) set up: a) test setup of the WST specimen, and b) free body diagram of forces [3].

## 2.2 Apparatus

The testing system used consisted of a loading frame, a load cell, two displacement measurement devices and data acquisition equipment:

- *Loading frame* – ELE Digital Tritest 100 (loading capacity 500kN) used under stroke control. *Load cell* – UtilCell 610 (nominal load 25 kN, linearity error <  $\pm 0.25\%$  F.S.) with signal conditioning amplifiers Krenel CEL/M010. *Displacement measuring devices* – Two LVDT displacement transducers RDP GT2500,  $\pm 2.5\text{mm}$  (linearity error <  $\pm 0.1\%$  F.S.), with signal conditioning amplifiers RDP S7AC, were used in the axis of the horizontal splitting force, one on each side of the specimen (COD1 on side 1, COD2 on side 2). *Data acquisition* – ELE automatic data acquisition unit.

## 2.3 Specimen configuration and dimensions

Cylindrical specimens were prepared by sawing a groove and a notch according to the geometry and dimensions indicated in Figure 2, where  $L$  is the ligament length and  $D$  the ligament depth. In order to force a straight crack propagation path, a 5 mm-deep groove was cut on both sides of the specimen, on the circular surfaces perpendicular to its axis (see perspective view in Figure 2).

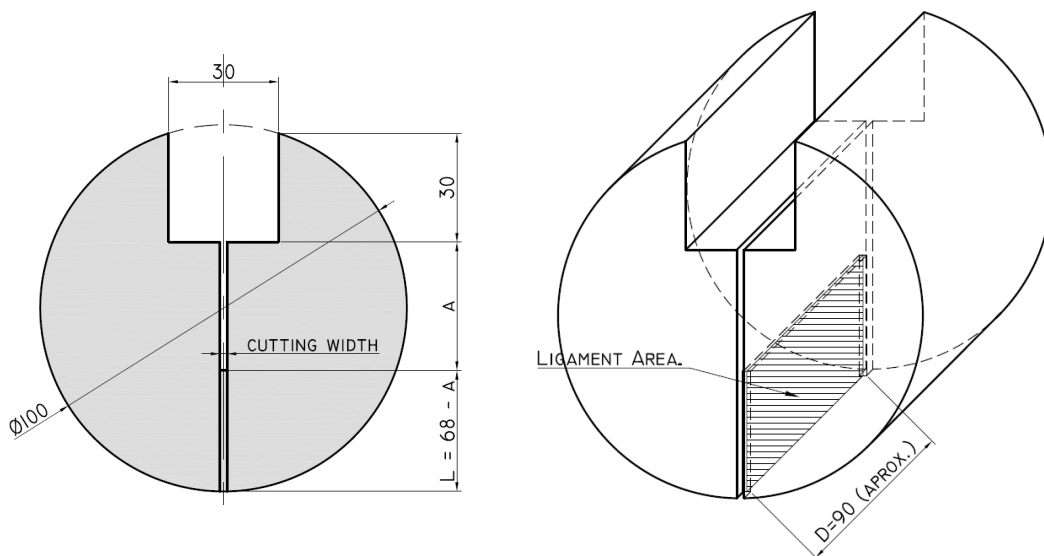


Figure 2: Dimensions of the WST specimen.

## 2.4 Materials

Two different types of rock were tested:

- *Lleida Sandstone*: It is a small-grained compact sandstone (calcarenite) obtained from a local quarry, with the following properties: Flexural Strength= 6.5 MPa, Apparent Density= 23.2 kN/m<sup>2</sup>, Open Porosity= 15%, Compression Strength= 50.3 MPa, Elastic Modulus= 15.6 GPa.
- *Reservoir Rock*: It is a calcareous rock from deep perforation cores of 100 mm

diameter. No physical properties of this rock were known at the moment of performing WST.

### 3 NUMERICAL MODELING OF THE WST

The model geometry and the mesh used are shown in Figure 3, where grey elements represent the rock, blue elements represent the steel loading plates and magenta elements represent an “equivalent spring” on behalf of the machine compliance. The notch (blue) and the fracture path (red) on the rock were represented by zero-thickness interface elements.

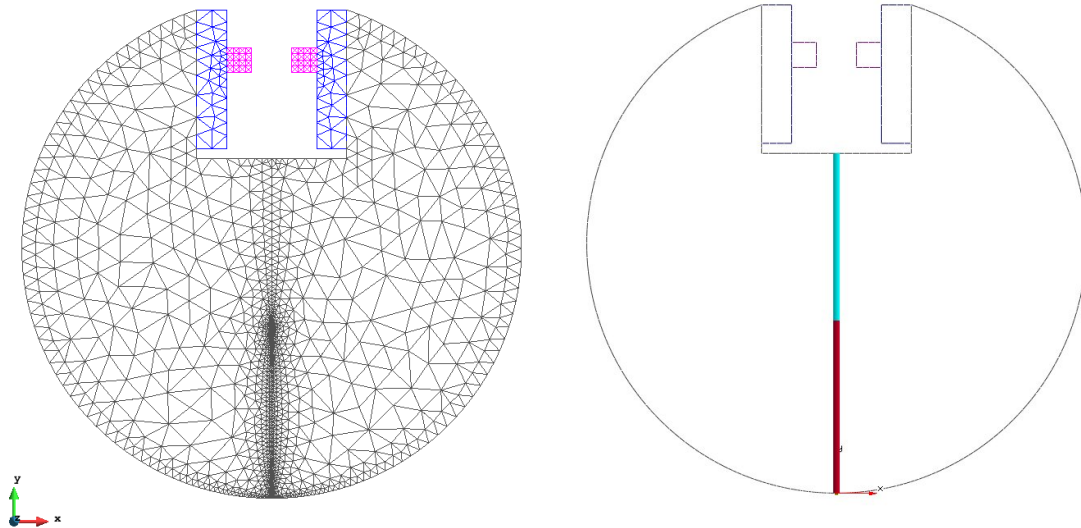


**Figure 3:** Finite element mesh, continuum elements (left) and interface elements (right).

The lower roller support was simulated by restricting the vertical displacement of the lowest nodes. The horizontal displacement imposed on the roller bearings by the testing machine was simulated by imposing horizontal displacements of same values and opposite sign, on the equivalent springs.

For continuum elements (rock, plates and equivalent spring), isotropic linear elastic materials were assumed. The interface elements representing the notch were equipped with a linear elastic constitutive law and very low elastic stiffness  $K_n$  and  $K_t$ , so that they do not oppose any significant resistance to opening. The constitutive model used for the interface elements along the fracture path was the elastoplastic constitutive model with fracture energy-based evolution laws described in detail in [4].

## 4 WST CONDUCTED ON LLEIDA SANDSTONE SPECIMENS

### 4.1 Experimental Results

A Lleida sandstone specimen with a ligament length  $L = 33$  mm and a ligament depth  $D = 94$  mm was tested. The  $P_H$ –COD curve obtained is plotted with grey circles in Figure 5. In order to make the curve comparable with others with different ligament depth, the load measurement has been normalized to a 1000 mm ligament depth by multiplying the original values by a factor  $1000/D$ . The specific fracture energy ( $G_f^I$ ) measured was 54.8 N/m. After

the test, the specimen exhibited a clean straight fracture path as shown in Figure 4.

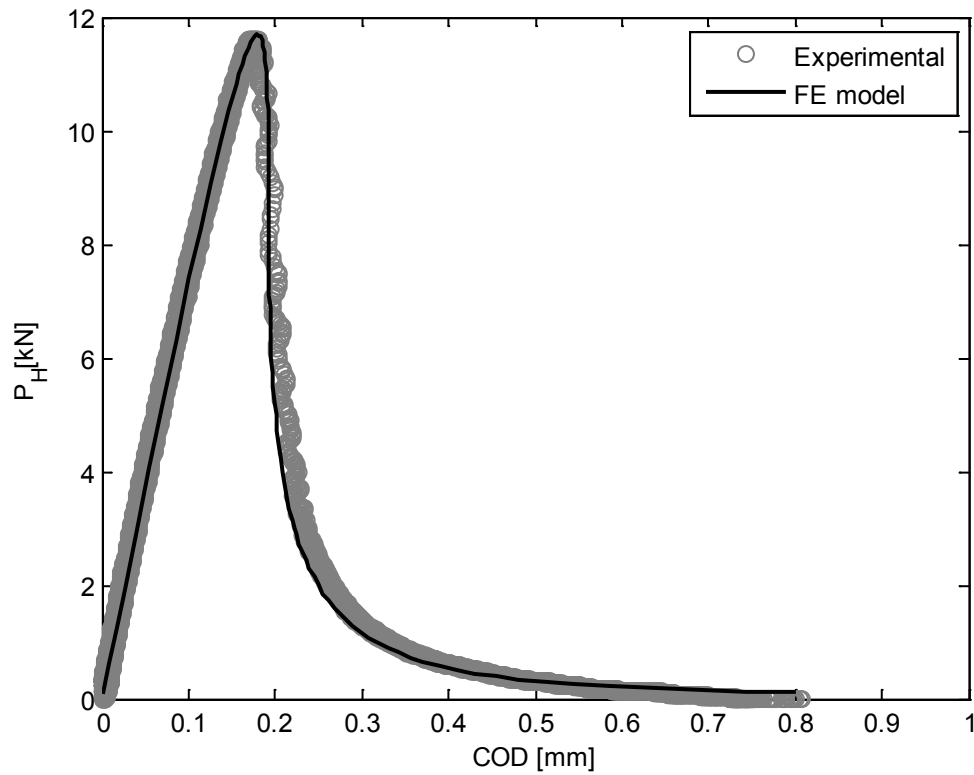


**Figure 4:** WST Horizontal Force ( $P_H$ ) – COD curves of alternative sandstone specimen, with a ligament length of  $L=33$  mm, obtained experimentally and from numerical simulation. The experimental curve has been normalized to a ligament depth of 1.

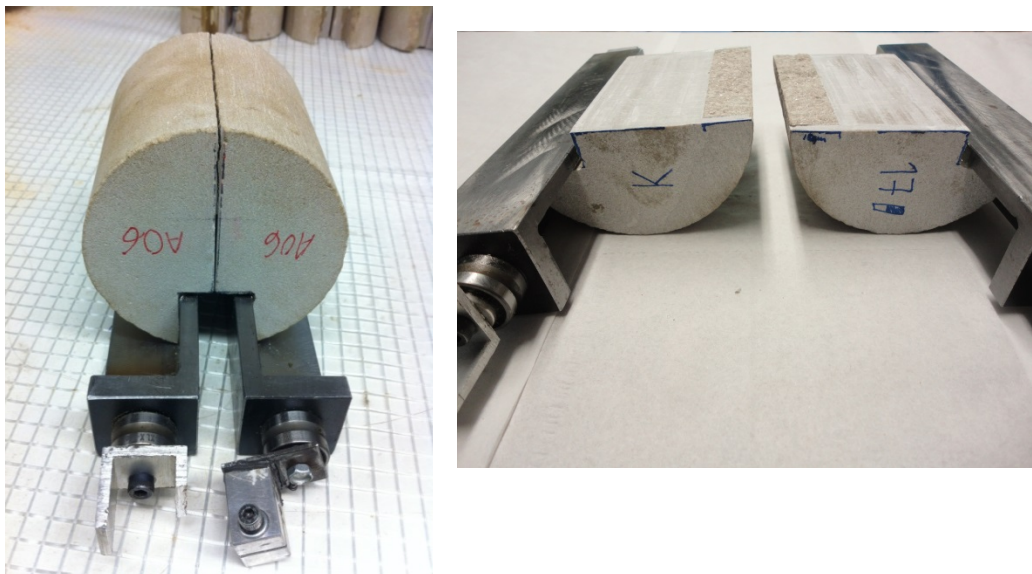


**Figure 5:** Specimens after test, Lleida sandstone (left), Reservoir rock (right).

## 4.2 Numerical Results

The experimental WST on Lleida sandstone was numerically simulated using the material parameters summarized in Tables 1 and 2. The tensile strength of the rock and the elastic modulus of the equivalent spring were estimated by fitting the  $P_H$ –COD curve shown in Figure 5. Note that the fitted tensile strength agrees very well with the flexural strength parameter that had been provided in advance by the quarry.

**Table 1:** Material properties of the continuum elements for Lleida sandstone analysis.

	Unit	Lleida sandstone	Steel plates	Equivalent spring
$E$ (Young’s modulus)	MPa	15600	200000	700
$\nu$ (Poisson’s ratio)	—	0.15	0.3	0

**Table 2:** Material properties of interface elements for Lleida sandstone analysis.

	Unit	Notch Interfaces	Fracture path Interfaces
$K_n$ (normal stiffness)	MPa/m	1.0	1.0E+09
$K_t$ (tangential stiffness)	MPa/m	1.0	1.0E+09
$\tan \phi$ (friction angle)	—	—	0.78 (38°)
$\chi$ (tensile strength)	MPa	—	6.5
$c$ (cohesion)	MPa	—	12.4
$G_f^I$ (fracture energy mode I)	MPa·m	—	54.8E-06
$G_f^{IIa}$ (fracture energy mode IIa)	MPa·m	—	54.8E-05

## 5. TESTS CONDUCTED ON RESERVOIR ROCK SPECIMENS

### 5.1 Experimental Results

A reservoir specimen was tested with a ligament length of 19.5 mm. The  $P_H$ –COD curve obtained is plotted in Figure 6 with grey circles. The specific fracture energy ( $G_f^I$ ) measured is 52.9 N/m. The specimen presented a straight fracture path as it is shown in Figure 4.

### 5.2 Numerical Results

The experimental WST on the reservoir rock specimen was numerically simulated using the material parameters summarized in Table 3 and Table 4. The tensile strength and the elastic modulus of the rock were adjusted by trial and error to 10 MPa and 45 GPa respectively, in order to fit the  $P_H$ –COD curve, as it is shown in Figure 5. The elastic modulus of the “equivalent spring” representing the stiffness of the testing machine was the same one identified with the quarry specimens in paragraph 4.2.

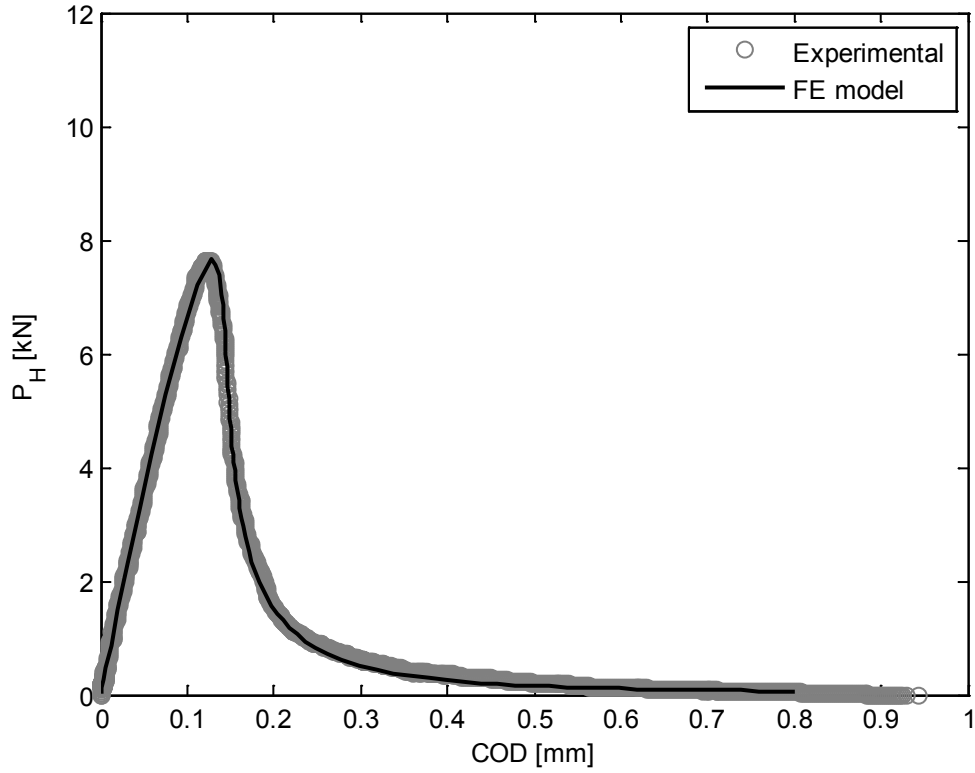


**Figure 6:** PH –COD curves from Repsol rock specimens obtained experimentally and from numerical simulation. Results normalized to a specimen depth of 1 m.

**Table 3:** Material properties of the continuum element for reservoir rock analysis.

	Unit	Reservoir rock	Steel plates	Equivalent spring
E (Young's modulus)	MPa	45000	200000	700
$\nu$ (Poisson's ratio)	-	0.15	0.3	0

**Table 4:** Material properties of the interface elements for reservoir rock analysis.

	Unit	Notch Interfaces	Fracture path Interfaces
$K_n$ (normal stiffness)	MPa/m	1.0	1.0E+09
$K_t$ (tangential stiffness)	MPa/m	1.0	1.0E+09
$\tan \phi$ (friction angle)	-	-	0.78 (38°)
$\chi$ (tensile strength)	MPa	-	10.0
$c$ (cohesion)	MPa	-	10.0
$G_f^I$ (fracture energy mode I)	MPa·m	-	52.9E-06
$G_f^{IIa}$ (fracture energy mode IIa)	MPa·m	-	52.9E-05

## 6 CONCLUDING REMARKS

Experimental results of Wedge Splitting Tests conducted on notched cylindrical specimens of two different types of rock have been presented. The numerical simulation of these tests using the FEM with fracture-based zero-thickness interface elements led to a very accurate simulation of the load –displacement tests, and turned out crucial for the planning of experimental work, including the estimate of the stiffness of the testing machine as well as other mechanical parameters of the rock such as young modulus and tensile strength.

## ACKNOWLEDGMENTS

The work was partially supported by research grants BIA2012-36898 from MEC (Madrid), which includes FEDER funds, and 2014SGR-1523 from Generalitat de Catalunya (Barcelona). The support from REPSOL for this research is also gratefully acknowledged. The first author acknowledges MICINN (Madrid) for his FPI doctoral fellowship.

## REFERENCES

- [1] Brühwiler, E. and Wittmann, F., “The wedge splitting test, a new method of performing stable fracture mechanics tests,” *Engineering Fracture Mechanics*, vol. 35, no. 1, pp. 117–125, 1990.
- [2] Saouma, V., Broz, J., Brühwiler, E. and Boggs, H., “Effect of aggregate and specimen size on fracture properties of dam concrete,” *J. Mater. Civ. Eng.*, vol. 3, no. 3, pp. 204–218, 1991.
- [3] Kumar, S. and Barai, S.V., *Concrete fracture models and applications*. Springer Science & Business Media, 2011.
- [4] Carol, I., Prat, P. and López, C.M., “Normal/Shear Cracking Model: Application to Discrete Crack Analysis,” *Journal of Engineering Mechanics*, vol. 123, no. 8, pp. 765–773, 1997.